Electronic Supplementary Information

Spray-drying-assisted Construction of Hierarchically Porous ZIF-8 for Controlled Release of Doxorubicin

Yan Wei,[a,b] Miao Chang,[b] Jingran Liu,[a,b] Ni Wang,[a,b] and Jie-Xin Wang[a,b*]

[a]*State Key Laboratory of Organic-Inorganic Composites, Beijing University of Chemical Technology, Beijing 100029, PR China*;

[b]*Research Center of the Ministry of Education for High Gravity Engineering and Technology, Beijing University of Chemical Technology, Beijing 100029, PR China*.

∗Corresponding author:
Jie-Xin Wang, E-mail: wangjx@mail.buct.edu.cn (J.X. Wang)

Experimental

Materials

Zinc nitrate hexahydrate ($Zn(NO_3)_2 \cdot 6H_2O$, 99 %) was purchased from Shanghai Aladdin Biochemical Technology Co., Ltd. 2-methyl imidazole (HmIM, 98 %) was bought from J&K Scientific Ltd. DOX hydrochloride (DOX·HCl, 98 %) and Phosphate Buffered Saline (PBS) were provided by Shanghai Yuanye Bio-Technology Co., Ltd. Organic solvents were purchased from Sinopharm Chemical Reagent Co., Ltd. Deionized water was obtained from a Hitech-K flow water purification system and used for all experiments. HeLa cells were bought from Shanghai Sangon Biotech Co., Ltd. Standard Cell Counting Kit-8 (CCK-8) was purchased from MCE Co., Ltd.

Preparation of HP-ZIF-8

Synthesis of N-ZIF-8: N-ZIF-8 with four different particle sizes (20, 30, 40 and 70 nm) were synthesized (denoted as N-ZIF-8-20, N-ZIF-8-30, N-ZIF-8-40 and N-ZIF-8-70). For N-ZIF-8-20, $Zn(NO_3)_2 \cdot 6H_2O$ (1.47 g) and 2-methylimidazole (3.24 g) were separately dissolved in methanol (200 mL). For N-ZIF-8-30, $Zn(NO_3)_2 \cdot 6H_2O$ (2.20 g) and 2-methylimidazole (4.87 g) were separately dissolved in methanol (200 mL). For N-ZIF-8-40, $Zn(NO_3)_2 \cdot 6H_2O$ (2.93 g) and 2-methylimidazole (6.49 g) were separately dissolved in methanol (200 mL).[1] With vigorous stirring, the metal salt solution was poured into the ligand solution at room temperature, the reaction times of N-ZIF-8-20, N-ZIF-8-30, and N- ZIF-8-40 were 60, 45, and 30 min, respectively. For N-ZIF-8-70, $Zn(NO_3)_2 \cdot 6H_2O$ (2.93 g) and 2-methylimidazole (3.24 g) were separately dissolved in methanol (200 mL). After complete mixing, the resulting solution was kept for 1 h without stirring followed by centrifugation.[1] All the wet particles

were washed and then transferred into deionized water to form aqueous suspensions.

Preparation of HP-ZIF-8: In a typical spray-drying process, by using deionized water as the solvent, four kinds of HP-ZIF-8 were prepared by spray drying in a spray dryer (B-290, BÜCHI Labortechnik AG, Switzerland) at the inlet temperature of 373 K, the feed rate of 15 mL min^{-1}, the flow rate of 536 L h^{-1} and the solid content of 2 wt%. The products were washed thoroughly with methanol to remove the unreacted metal ions and ligands within the pores and further heated in vacuum at 423 K for 12 h. The preparation process of HP-ZIF-8 and the spray-drying system are shown in Scheme S1.

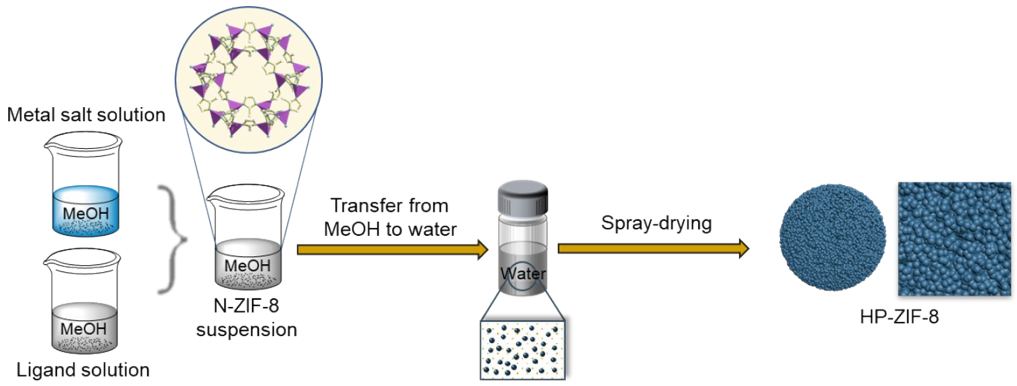

Scheme S1 Schematic illustration of the preparation of HP-ZIF-8.

Preparation of DOX@HP-ZIF-8

Firstly, DOX was added to the ZIF-8 suspension in deionized water with a solid content of 2 wt%. Activated N-ZIF-8 wet particles were used in this process to prevent reactants from participating in the subsequent steps, which may affect the physicochemical properties of the drug. After the mixture was sonicated for 3 min and DOX was completely dissolved, spray drying was carried out under the same preparation condition as that of HP-ZIF-8. Samples were collected and further washed with DI water three times, followed by freeze-drying to remove the residual solvent. The preparation process of DOX@HP-ZIF-8 is shown in Scheme S2.

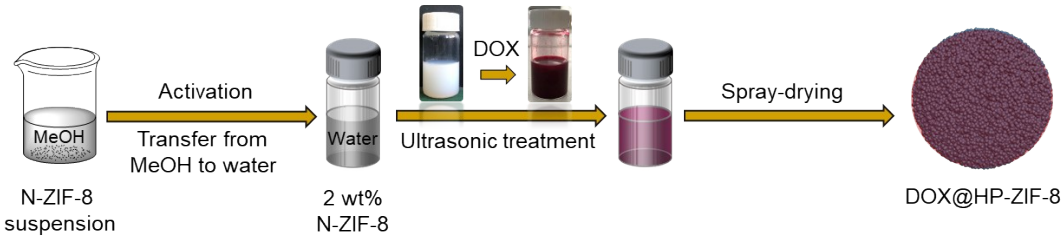

Scheme S2 Schematic illustration of the preparation of DOX@HP-ZIF-8.

Control experiments

With the same theoretical DOX loading of 50 wt%, DOX-loaded N-ZIF-8-40 and HP-ZIF-8-40 (denoted as DOX&N-ZIF-8 and DOX&HP-ZIF-8) were prepared by a solvent adsorption approach and compared with the spray-dried DOX@HP-ZIF-8.

DOX&N-ZIF-8: 50 mg powder N-ZIF-8-40 was suspended in deionized water (10 mL) and sonicated for 10 min. DOX (50 mg) was then added to the above suspension with stirring for 24 h followed by centrifugation and washing, and further freeze-dried to remove the residual solvent.

DOX&HP-ZIF-8: 50 mg powder HP-ZIF-8-40 was suspended in deionized water (10 mL) and stirred for 10 min. DOX (50 mg) was then added to the above suspension with stirring for 24 h followed by centrifugation and washing, and further freeze-dried to remove the residual solvent.

Characterization

The structure and crystal phase of materials were checked by powder X-ray diffraction (PXRD) measurement performed on a D8 Advance X diffractometer equipped with a Cu sealed tube (λ = 1.54178 Å). The particle sizes of N-ZIF-8 were imaged by transmission electron microscopy (TEM, Hitachi HT-7700), and the morphologies of hierarchically porous structures were measured by field emission scanning electron microscopy (FESEM, JEOL JSM-7800F).

The specific surface areas and the pore size contributions were estimated based on the N_2 isotherms at 77 K measured by an automatic surface and aperture analyzer (Beishide 3H-2000PS2) through the Brunauer-Emmett-Teller (BET) and Barrett-Joyner-Halenda (BJH) model respectively. The loading of DOX was qualitatively analyzed by Fourier transform infrared spectroscopy (FTIR, Bruker Vertex 70). The localization of DOX in DOX@HP-ZIF-8 was observed by an optical microscope (OM, Yujie YJ-2016). The thermal and structural stability were performed by thermogravimetric analysis (TGA, RIGAKU Thermo plus EVO2). The concentration of DOX was recorded using an ultraviolet-visible spectrophotometer (UV-vis, SHIMADZU UV2600). The CCK-8 results were obtained by a microplate reader (BioTek Epoch2) at 450 nm and the cell images were collected by an inverted fluorescence microscope (OLYMPUS IX73P1F).

DOX loading capacity and encapsulation efficiency

The amount of DOX encapsulated with samples was determined from the UV-vis absorbance at 479 nm after the samples have been completely dissolved in an acidic medium.[2] 2 mg sample was dissolved in 5 mL HCl solution. According to the standard curve of DOX, after the complete decomposition of ZIF-8, DOX concentration was determined by UV/Vis, while calculating the practical loading of DOX.

DOX loading capacity:

$$Theoretical\ loading\ of\ DOX(\%) = \frac{m_{\text{DOX-added}}}{m_{\text{ZIF-8}}} \times 100\% \quad (1)$$

$$Practical\ loading\ of\ DOX(\%) = \frac{m_{\text{DOX-loaded}}}{m_{\text{ZIF-8}}} \times 100\% = = \frac{m_{\text{DOX-loaded}}}{m_{\text{ZIF-8+DOX-loaded}}} \times 100\% \quad (2)$$

Encapsulation efficiency:

$$Encapsulation\ efficiency(\%) = \frac{m_{\text{DOX-loaded}}}{m_{\text{DOX-added}}} \times 100\% \quad (3)$$

***In vitro* release of DOX**

The release of DOX from samples was monitored in PBS buffer solution at 37℃ under gentile shaking with a frequency of 100 rpm. In brief, 10 mL of sample (1 mg mL^{-1}) was transferred to a presoaked dialysis cassette (10-kDa cutoff, Yuanye Shanghai) and immersed in the release medium. At predetermined time intervals, 3 mL of release buffer was removed and followed by measurement, and the corresponding fresh buffer solution (3 mL) was added back into the system. For free DOX, DOX powder (1.67 mg) in an amount equal to the theoretical DOX mass in DOX@HP-ZIF-8 was added to a 10 mL buffer solution for dissolution and then transferred to a presoaked dialysis cassette. The concentration of released DOX was determined with UV characterization.

The release percentages of DOX were calculated according to the following equation:

$$DOX(\%) = (C_t V_{total} + \sum_{0}^{t\text{-}1} C_t V_t) / m_l \times 100\% \quad (4)$$

where C_t (mg mL^{-1}) is the concentration of DOX release from DOX@HP-ZIF-8 at time t, V_{total} is the fixed total volume (200 mL) of PBS buffer solution, V_t is the certain volume (3 mL) of the release buffer taken out at time t, and m_l is the total amount of loaded DOX.

The release data were fitted with the zero-order, first-order, Higuchi, and Ritger-Peppas models as follows:[3-5]

$$\frac{M_t}{M_\infty} = kt + b \quad (5)$$

$$\frac{M_t}{M_\infty} = 1\text{-}e^{-kt} \quad (6)$$

$$\frac{M_t}{M_\infty} = kt^{0.5} + b \quad (7)$$

$$\frac{M_t}{M_\infty} = kt^n \quad (8)$$

where M_t/M_∞ is the release percentage of DOX release from DOX@HP-ZIF-8 at time t, k is the rate constant, and n is the diffusion parameter.

Cell culture

HeLa cells were cultured in Dulbecco's Modified Eagles Medium (DMEM) supplemented with 10% Fetal Bovine Serum (FBS) and 1% streptomycin at 37 ℃ with 5% CO_2 in the atmosphere.

Cellular uptake

To investigate the cell uptake of the DOX@HP-ZIF-8-40, HeLa cells were seeded into laser confocal dishes and incubated for 24 h. Then, the sample solution/suspensions (in DMSO, at DOX concentration of 1 μg ml^{-1}) were introduced to the dishes and further incubated for 2 h. After removing the medium, the cells were washed with PBS at least three times and imaged by an inverted fluorescence microscope.

***In vitro* cytotoxicity study**

CCK-8 assay was conducted to investigate the cytotoxicity of HP-ZIF-8-40 and the anticancer efficiency of the DOX@HP-ZIF-8-40. Firstly, HeLa cells were seeded into 96-well plates at a density of 1×10^4 cells $well^{-1}$ and incubated for 24 h. Afterward, the medium was

replaced with fresh PBS followed by the addition of HP-ZIF-8-40 and DOX@HP-ZIF-8-40 with various concentrations to each group (three wells), respectively. After further incubation for 24 and 72 h, the cell was incubated in different 110 μL of DMEM containing 10 μL Cell Counting Kit-8 (CCK-8) solution for 2 h. The absorbance of the suspension was determined with a microplate reader at 450 nm.

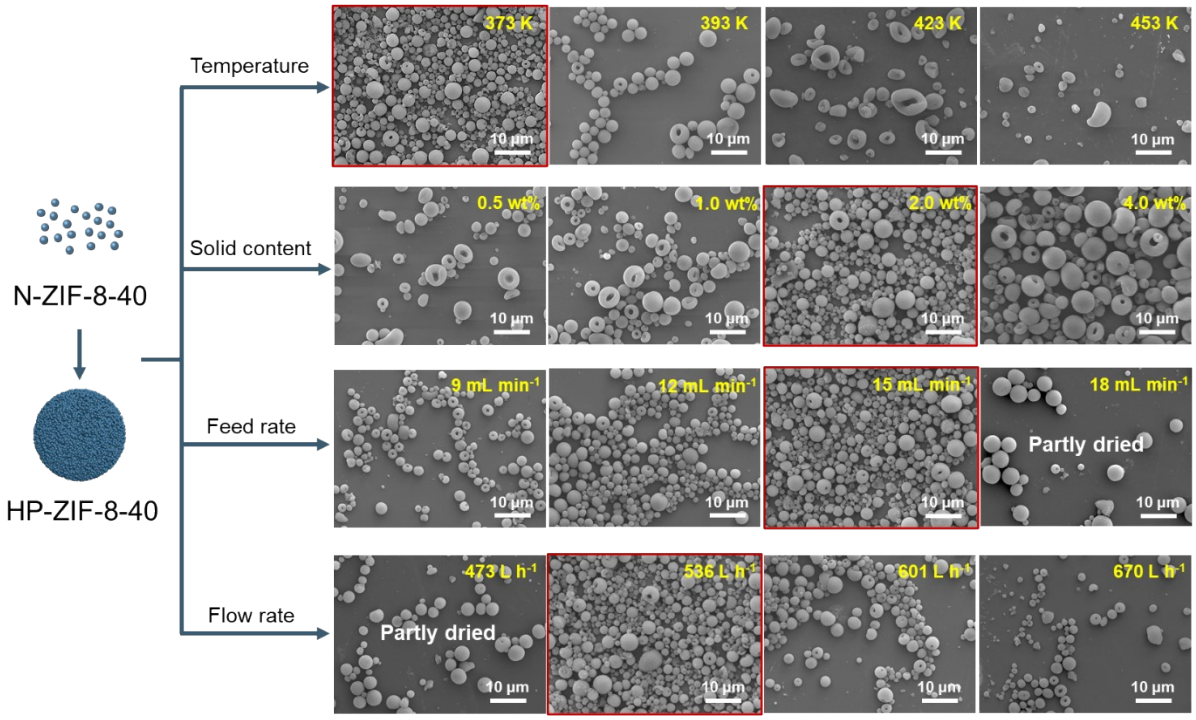

Fig. S1 FESEM images of HP-ZIF-8-40 prepared at different spray-drying conditions. (Solvent is DI water, inlet temperature is 373 K, solid content is 2.0 wt%, feed rate is 15 mL $min^{-1,}$ and flow rate is 536 L h^{-1})

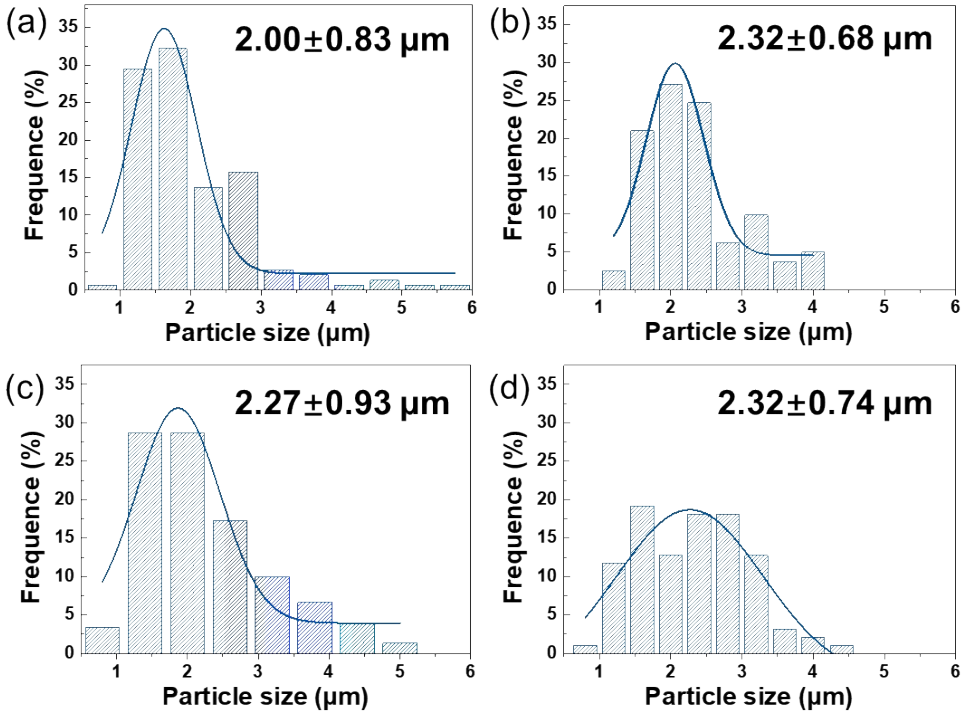

Fig. S2 Particle size distributions of HP-ZIF-8 with different primary particle sizes: (a) 20 nm, (b) 30 nm, (c) 40 nm, (d) 70 nm.

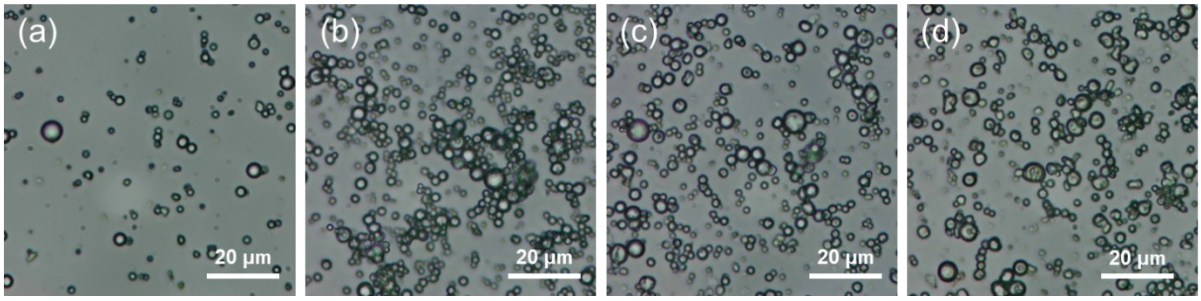

Fig. S3. Optical microscope images of HP-ZIF-8 with different primary particle sizes: (a) 20 nm, (b) 30 nm, (c) 40 nm, (d) 70 nm.

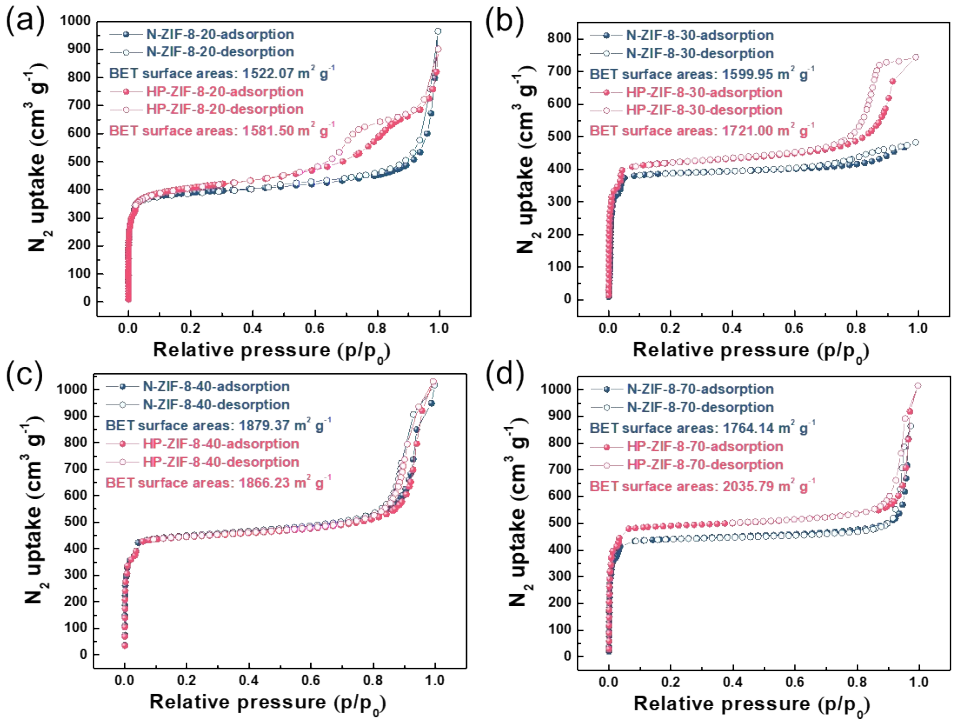

Fig. S4 77 K N_2 adsorption-desorption isotherms of N-ZIF-8 and HP-ZIF-8 with primary particle sizes: (a) 20 nm, (b) 30 nm, (c) 40 nm, (d) 70 nm.

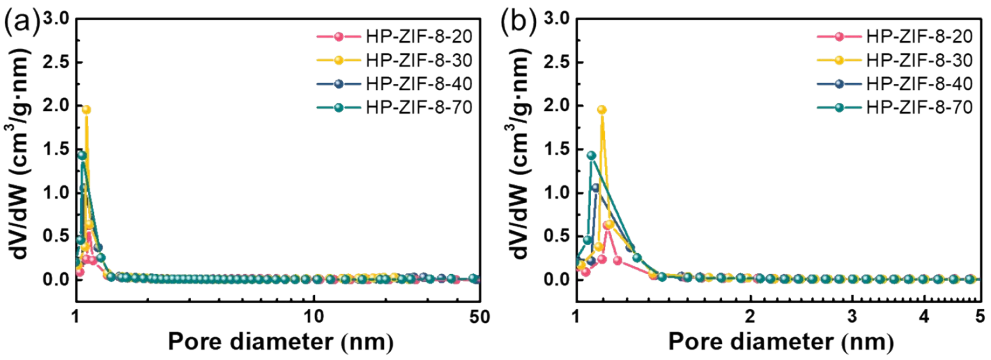

Fig. S5 Pore size distributions of HP-ZIF-8 obtained using the NLDFT model.

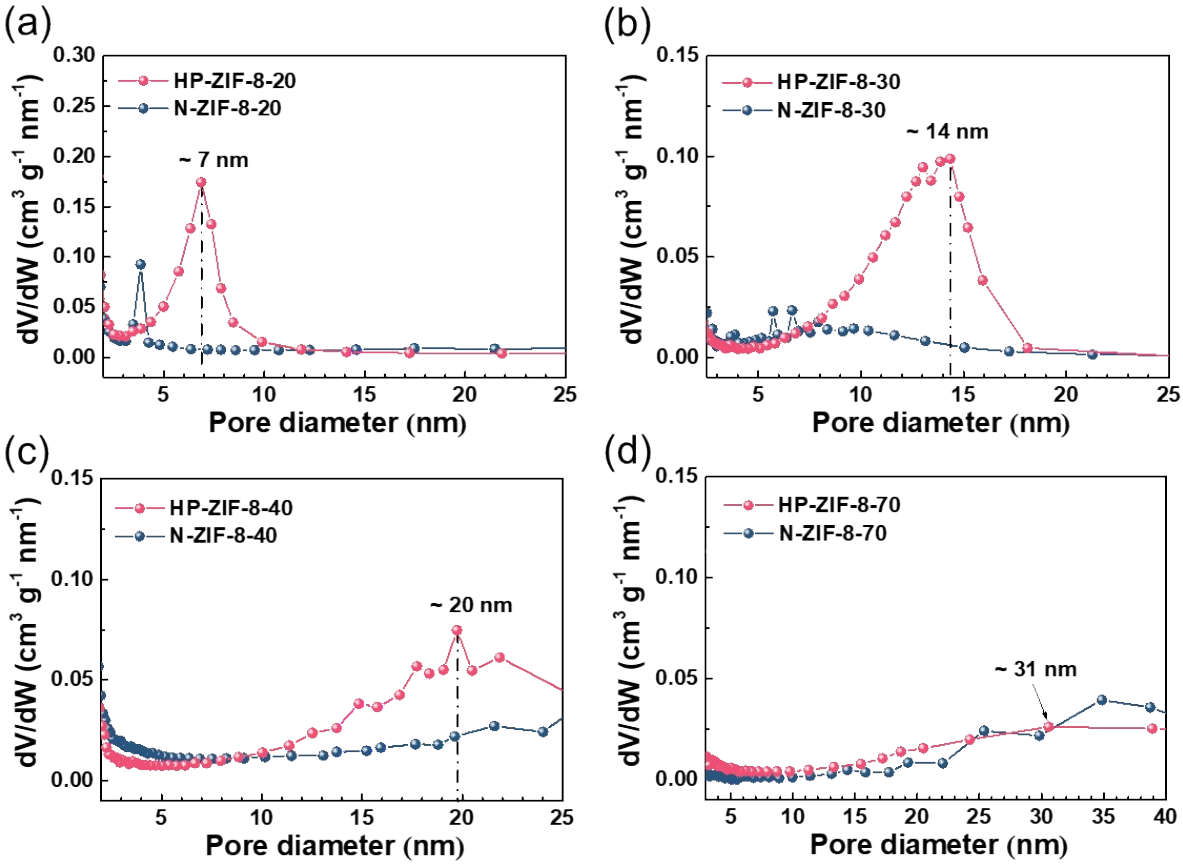

Fig. S6 Pore size distributions of N-ZIF-8 and HP-ZIF-8 with different primary particle sizes: (a) 20 nm, (b) 30 nm, (c) 40 nm, (d) 70 nm.

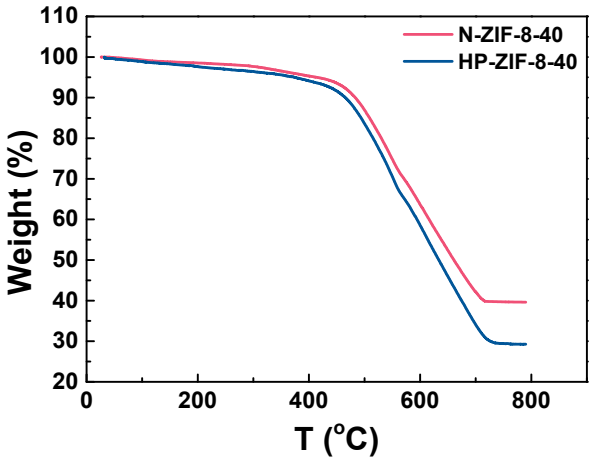

Fig. S7 TGA curves of N-ZIF-8-40 and HP-ZIF-8-40.

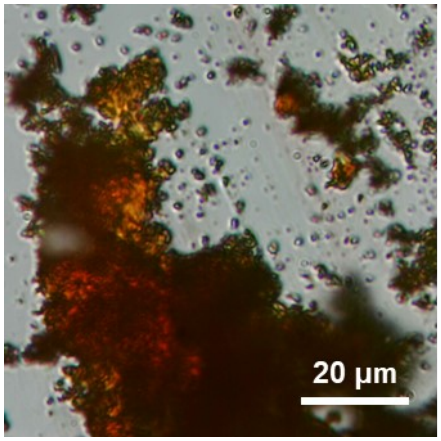

Fig. S8 Optical microscopic image of DOX.

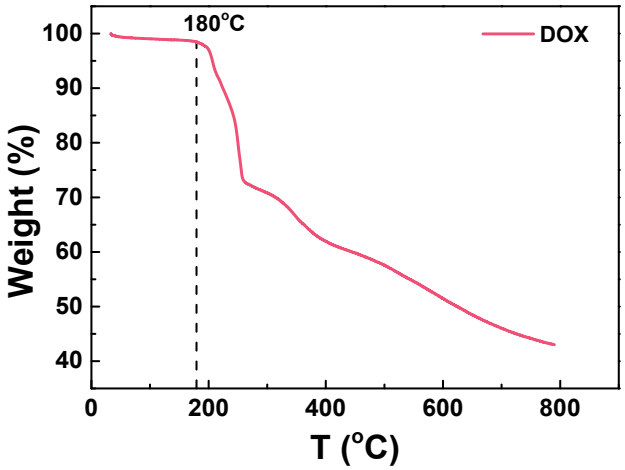

Fig. S9 TGA curve of DOX.

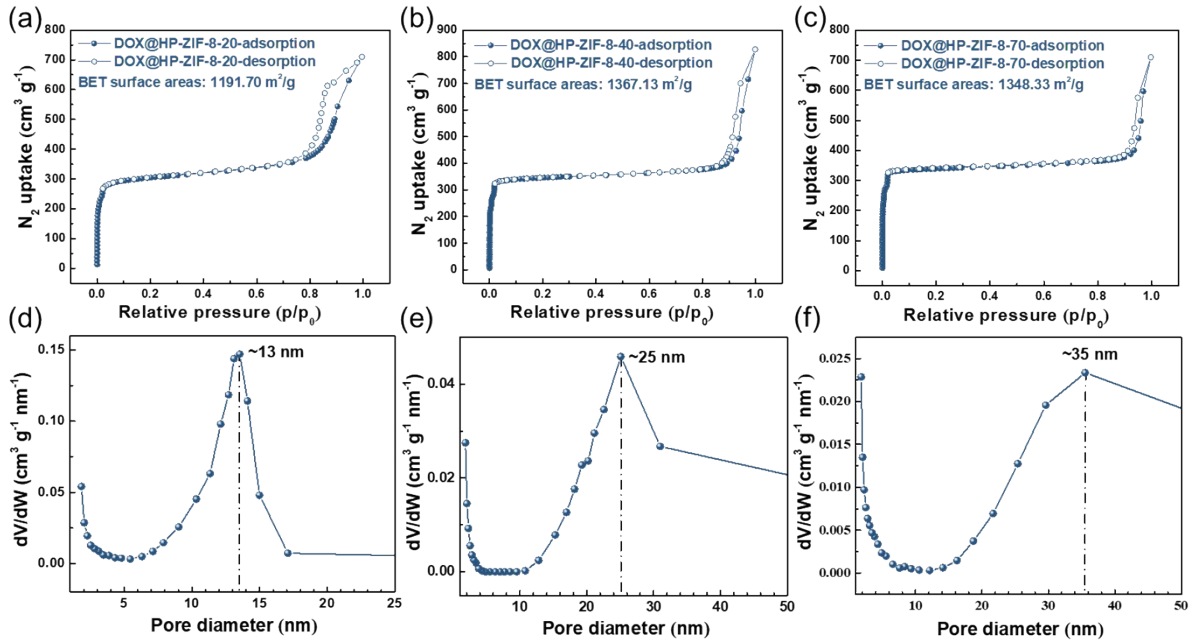

Fig. S10 77 K N_2 adsorption-desorption isotherms and pore size distribution curves of DOX@HP-ZIF-8 with different primary particle sizes: (a, d) 20 nm, (b, e) 40 nm, (c, f) 70 nm.

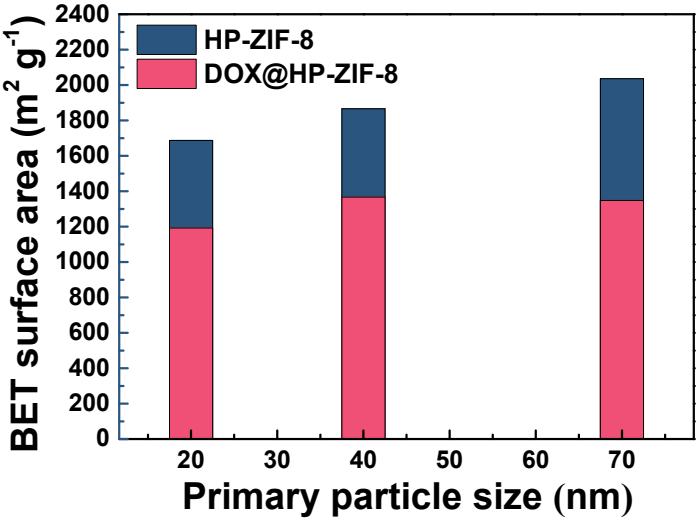

Fig. S11 BET surface areas of HP-ZIF-8 and DOX@HP-ZIF-8 with different primary particle sizes.

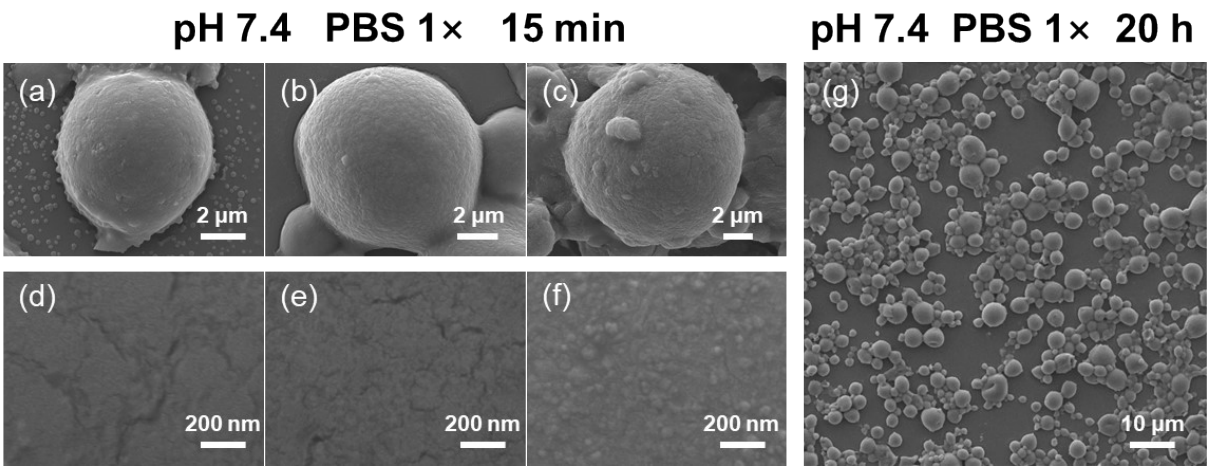

Fig. S12 FESEM images of DOX@HP-ZIF-8 with different primary particle sizes: (a, d) 20 nm, (b, e) 40 nm, (c, f) 70 nm in PBS buffer solution (pH 7.4) for 15 min; (g) FESEM image of DOX@HP-ZIF-8-40 in PBS buffer solution (pH 7.4) for 20 h.

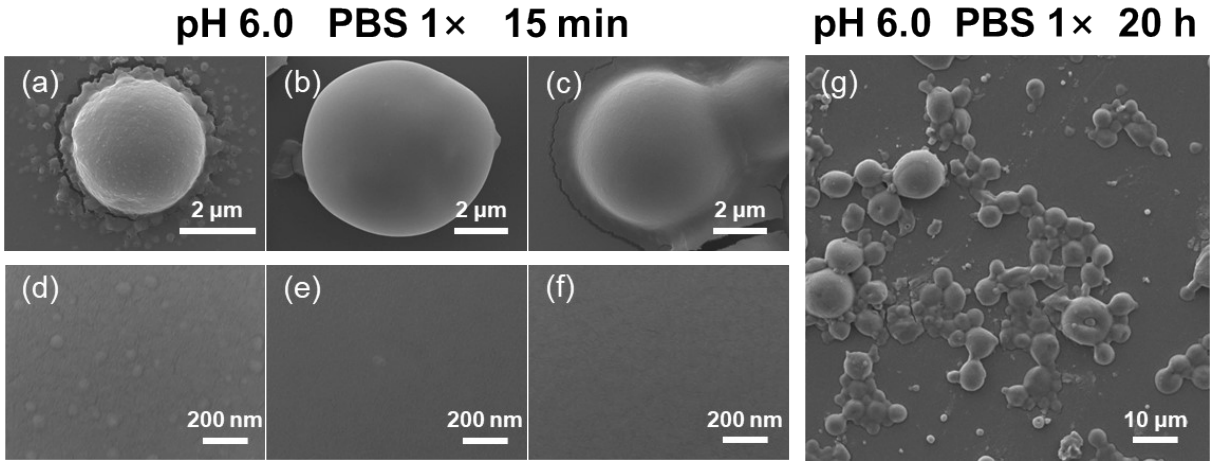

Fig. S13 FESEM images of DOX@HP-ZIF-8 with different primary particle sizes: (a, d) 20 nm, (b, e) 40 nm, (c, f) 70 nm in PBS buffer solution (pH 6.0) for 15 min; (g) FESEM image of DOX@HP-ZIF-8-40 in PBS buffer solution (pH 6.0) for 20 h.

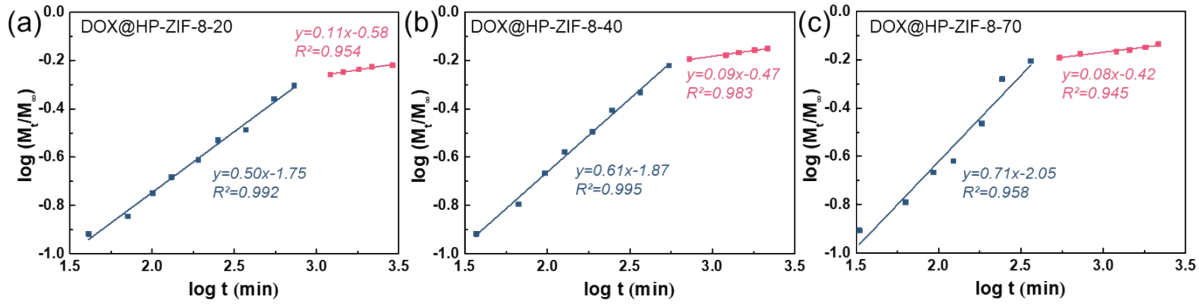

Fig. S14 Plots of log (M_t/M_∞) against log t of DOX@HP-ZIF-8 with different primary sizes (pH 6.0): (a) 20 nm, (b) 40 nm, (c) 70 nm.

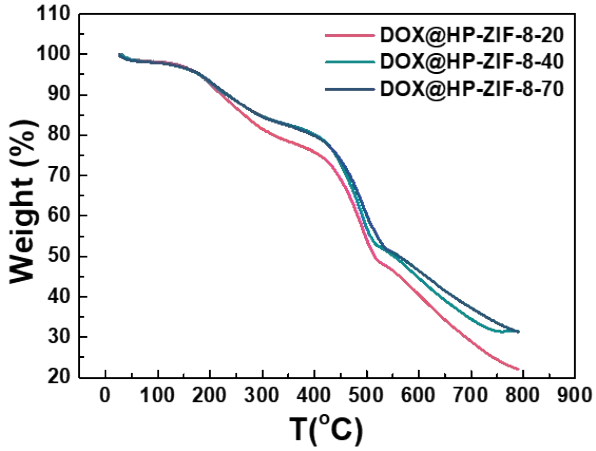

Fig. S15 TGA curves of DOX@HP-ZIF-8.

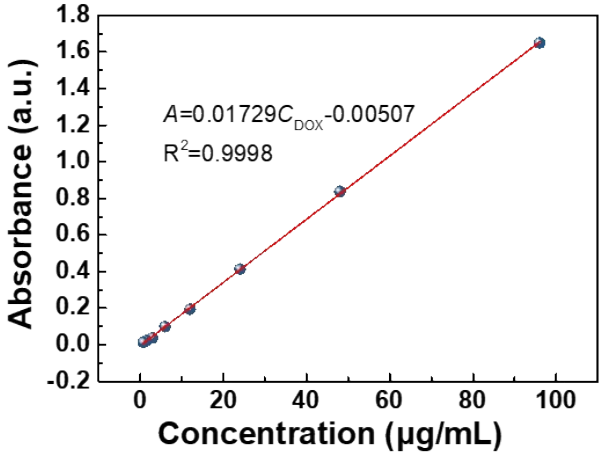

Fig. S16 Standard curve of DOX.

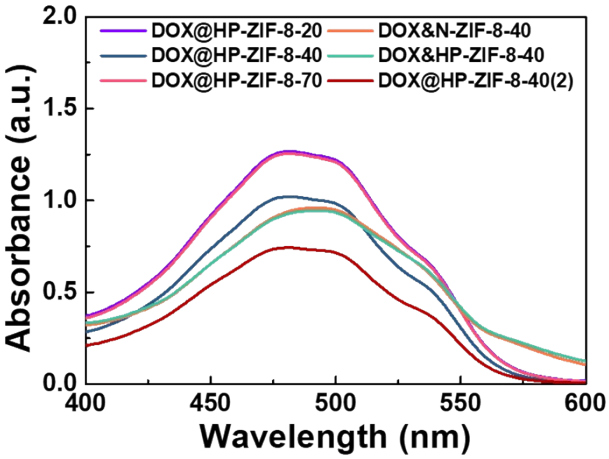

Fig. S17 UV-vis spectra of synthesized samples after completely dissolved in an acidic medium.

Table S1 Theoretical and practical loading of DOX molecules encapsulated with ZIF-8.

Sample	Theoretical loading of DOX molecules (%)	Practical loading of DOX molecules (%)
DOX@HP-ZIF-8-20	20	20.90
DOX@HP-ZIF-8-40	20	18.17
DOX@HP-ZIF-8-70	20	18.94
DOX&N-ZIF-8-40	100	22.64
DOX&HP-ZIF-8-40	100	25.52
DOX@HP-ZIF-8-40	100	79.05

Table S2 The corresponding UV-Vis data and calculated values.

Sample	Absorbance	m_{sample} (mg)	C_{DOX} (μg mL^{-1})	V_{HCl} (mL)	m_{DOX} (mg)
DOX@HP-ZIF-8-20	1.268	2.13	73.63	5	0.37
DOX@HP-ZIF-8-40	1.021	1.93	59.34	5	0.30
DOX@HP-ZIF-8-70	1.256	2.29	72.94	5	0.36
DOX&N-ZIF-8-40	0.959	1.51	55.76	5	0.28
DOX&HP-ZIF-8-40	0.944	1.35	54.89	5	0.27
DOX@HP-ZIF-8-40(2)	0.743	1.96	43.27	20	0.87

Table S3 Relative proportions of atomic in DOX, HP-ZIF-8-40, and DOX@HP-ZIF-8-40.

	DOX	HP-ZIF-8-40	DOX@HP-ZIF-8-40
C1s	71.07	56.62	58.23
N1s	3.17	23.29	19.23
O1s	25.76	3.65	9.72
Zn2p		8.16	6.02

Table S4 Correlation coefficients from fitting four mathematical models to the release curves of DOX from DOX@HP-ZIF-8 under different pH conditions.

Model	R^2					
	DOX@HP-ZIF-8-20		DOX@HP-ZIF-8-40		DOX@HP-ZIF-8-70	
	pH 7.4	pH 6.0	pH 7.4	pH 6.0	pH 7.4	pH 6.0
Zero-order model	0.7503	0.7229	0.6911	0.6922	0.7119	0.5839
First-order model	0.6833	0.6226	0.6171	0.5629	0.6290	0.4676
Higuchi equation	0.9236	0.9152	0.8921	0.8896	0.9123	0.8009
Ritger-Peppas equation	0.9813	0.9413	0.9705	0.9102	0.9817	0.8225

Table S5 Fitting results for DOX release curves of DOX&N-ZIF-8, DOX&HP-ZIF-8, and DOX@HP-ZIF-8 (pH 6.0).

Sample	Kinetic equation	R^2
DOX&N-ZIF-8	$M_t/M_\infty=2.68\ t^{0.35}$	0.9646
DOX&HP-ZIF-8	$M_t/M_\infty=2.47\ t^{0.33}$	0.9894
DOX@HP-ZIF-8	$M_t/M_\infty=1.92\ t^{0.35}$	0.9933

Table S6 Comparison of the DOX loading capacity and encapsulation efficiency with MOFs particles/composites.

Material	Method	Feed ratio (material:drug)	Loading capacity (%)	Encapsulation efficiency (%)	Ref
HP-ZIF-8-40	Spray-drying	5:1	20.9	~100	**This work**
		1:1	79.1	79.1	
ZIF-8	Adsorption	1:3	4.9	1.6	6
ZIF-8	One-pot method	5:1	20	~100	7
Zn(bix)	One-pot method	3:1	7	21	8
Filamentous ZIF-8	Adsorption	1:5	350	70	9
PCN-222	Adsorption	1:2	109	54.5	10
H-PMOF(PCN-222)	Adsorption	1:6	485	80.8	11
Mi-UiO-68	Adsorption	2:1	5.1	10.2	12
MIL-101-N_3(Fe)	Adsorption	2:5	15.4	6.2	13
PAA@ZIF-8	Adsorption	1:2	190	95	14
Fe_3O_4@ZIF-8	Adsorption	2.3:1	33	76.6	15
CuS@Fe-MOF	Adsorption	4:3	38	50.7	16
CS/Bio-MOF	Adsorption	1:1	36	36	17

References

1 J. Sánchez-Laínez, B. Zornoza, S. Friebe, J. Caro, S. Cao, A. Sabetghadam, B. Seoane, J. Gascon, F. Kapteijn, C. Le Guillouzer, G. Clet, M. Daturi, C. Téllez and J. Coronas, *J. Membr. Sci.*, 2016, **515**, 45-53.

2 H. Zheng, Y. Zhang, L. Liu, W. Wan, P. Guo, A. M. Nyström and X. Zou, *J. Am. Chem. Soc.*, 2016, **138**, 962-968.

3 Y. Cao, L. Huang, J. Chen, J. Liang, S. Long and Y. Lu, *Int. J. Pharmaceut.*, 2005, **298**, 108-116.

4 C. Chen, G. Zhang, Z. Dai, Y. Xiang, B. Liu, P. Bian, K. Zheng, Z. Wu and D. Cai, *Chem. Eng. J.*, 2018**,** ***349***, 101-110.

5 P. L. Ritger and N. A. Peppas, *J. Control Release*, 1987, **5**, 37-42.

6 I. B. Vasconcelos, T. G. d. Silva, G. C. G. Militão, T. A. Soares, N. M. Rodrigues, M. O. Rodrigues, N. B. d. Costa, R. O. Freire and S. A. Junior, *RSC Adv.*, 2012, **2**, 9437-9442.

7 H. Zheng, Y. Zhang, L. Liu, W. Wan, P. Guo, A. M. Nyström and X. Zou, *J. Am. Chem. Soc.*, 2016, **138**, 962-968.

8 I. Imaz, M. Rubio-Martínez, L. García-Fernández, F. García, D. Ruiz-Molina, J. Hernando, V. Puntes and D. Maspoch, *Chem. Commun.*, 2010, **46**, 4737-4739.

9 H. Yu, X. Qiu, P. Neelakanda, L. Deng, N. M. Khashab, S. P. Nunes and K.-V. Peinemann, *Sci. Rep.*, 2015, **5**, 15275.

10 W. Liu, Y.-M. Wang, Y.-H. Li, S.-J. Cai, X.-B. Yin, X.-W. He and Y.-K. Zhang, *Small*, 2017, **13**, 1603459.

11 X. Sun, G. He, C. Xiong, C. Wang, X. Lian, L. Hu, Z. Li, S. J. Dalgarno, Y.-W. Yang and J. Tian, *ACS Appl. Mater. Interfaces*, 2021, **13**, 3679-3693.

12 Y.-A. Li, X.-D. Zhao, H.-P. Yin, G.-J. Chen, S. Yang and Y.-B. Dong, *Chem. Commun.*, 2016, **52**, 14113-14116.

13 A. Bhattacharjee, M. K. Purkait and S. Gumma, *J. Inorg. Organomet. P.*, 2020, **30**, 2366-2375.

14 C. Zheng, Y. Wang, S. Z. F. Phua, W. Q. Lim and Y. Zhao, *ACS Biomater. Sci. Eng.*, 2017, **3**, 2223-2229.

15 N. Gong, X. Teng, J. Li and X.-J. Liang, *ACS Appl. Mater. Interfaces*, 2019, **11**, 37-42.

16 Z. Wang, W. Yu, N. Yu, X. Li, Y. Feng, P. Geng, M. Wen, M. Li, H. Zhang and Z. Chen, *Chem. Eng. J.*, 2020, **400**, 125877.

17 R. Abazari, A. R. Mahjoub, F. Ataei, A. Morsali, C. L. Carpenter-Warren, K. Mehdizadeh and A. M. Z. Slawin, *Inorg. Chem.*, 2018, **57**, 13364-13379.